A Note on The Discrete Binary Mumford-Shah Model

Jérôme Darbon *

Department of Mathematics, University of California (UCLA)
Los Angeles, CA Box 90095, USA.
jerome@math.ucla.edu

Abstract. This paper is concerned itself with the analysis of the two-phase Mumford-Shah model also known as the *active contour without edges* model introduced by Chan and Vese. It consists of approximating an observed image by a piecewise constant image which can take only two values. First we show that this model with the L^1-norm as data fidelity yields a contrast invariant filter which is a well known property of morphological filters. Then we consider a discrete version of the original problem. We show that an inclusion property holds for the minimizers. The latter is used to design an efficient graph-cut based algorithm which computes an exact minimizer. Some preliminary results are presented.

1 Introduction

The Mumford-Shah functional is a well-known model for image segmentation but its minimization is also a difficult task [2, 26]. Many models based on this functional have been proposed [12, 31]. Most of them consist of assuming that the segmented image is piecewise constant [26]. In particular the active contour without edges (ACWE) model, described by Chan and Vese in [12], consists of approximating an image with another image which can take only two values with an additional smoothness constraint. The latter is still difficult to optimize exactly. In this paper we shed new light on the analysis of the two-phase Mumford-Shah model (or ACWE) along with a new algorithm which computes an exact global minimizer.

Assume v is an observed image defined on Ω, a subset of $\mathbb{R}^2$ which takes values in $\mathbb{R}$. We intend to approximate v with an image which can take only two values μ_0 or μ_1. Let us denote by Ω_1 the set of the pixels of the image u that takes the value μ_1, i.e., $\Omega_1 = \{x \in \Omega \,|\, u(x) = \mu_1\}$. The energy E associated to

* Part of this work has been done while the author was with EPITA Research and Development Laboratory (LRDE), 14-16 rue Voltaire, F-9427 Le Kremlin-Bictre France. This work was also supported by grants from the ONR under contracts ONR N00014-06-1-0345, the NIH from the grant NIH U54-RR021813 and the NSF from grant NSF DMS-0610079.

the two-phase Mumford-Shah segmentation model is defined as follows :

$$\begin{aligned} E(\Omega_1, \mu_0, \mu_1 | v) = \beta\, Per\,(\Omega_1) & \\ + \int_{\Omega \setminus \Omega_1} f(\mu_0, v(x)) dx & \\ + \int_{\Omega_1} f(\mu_1, v(x)) dx \ , & \end{aligned} \tag{1}$$

where $Per(A)$ stands for the perimeter of the set A and where β is a weighted positive coefficient. Generally we have that $f(\mu_1, v(x)) = f(\mu_1 - v(x))$ and f is a *convex* function. For instance, f may be a power of a norm, i.e, $f(\cdot) = \| \cdot \|^p$ with $p \geq 1$.

Most of the available algorithms which minimize energy (1) either solve a system of coupled partial differential equations or perform alternate minimizations first for Ω_1, then for (μ_0, μ_1), and iterate until convergence to a local minimizer. The second optimization for (μ_1, μ_2) is not an issue [12]. However, the first one is difficult since it is a non-convex minimization problem [11]. For this one, the most popular methods rely on a level set formulation [12, 27, 31]. We refer the reader to [30] and the recent work of [23] for efficient level set based optimization. Nonetheless if one assume that the two values μ_0 and μ_1 are fixed, then one can compute a global minimizer by following the work of [11]. It consists in mapping the original non-convex problem into a convex one via the use of the Total Variation. Thus the problem reduces to perform an energy minimization with the Total Variation as the smoothness term. Many algorithms have been devoted to perform this minimization. Such an approach has also been applied in [7] to solve the active contour model.

If the support Ω is discretized then minimization over Ω_1 can be performed efficiently and exactly using graph-cut techniques [6, 20, 25] (See section 4). However, a straightforward application of these approaches to optimize over (Ω_1, μ_0) (or equivalently over (Ω_1, μ_1)) fails. This is one of the goals of this paper.

The main contributions of this paper are the following: first we show that if the data fidelity is modelled via the L^1 norm, i.e, $f(\cdot) = |\cdot|$, then minimization of the energy (1) defines a filter invariant by a change of contrast. The latter is a well known property of morphological filter [22, 29] Then, we consider a discrete version of the two-phase Mumford-Shah model. We show an inclusion property of the minimizers of this discrete energy. The latter is used to propose an efficient algorithm which computes an exact minimizer. To our knowledge these results are new. The structure of this paper is as follows. In Section 2 we show the morphological behavior of the model using a L^1 data fidelity term. In Section 3 we describe some optimality results. The latter are used to design our new minimization algorithm that is presented in Section 4 along with some preliminary numerical results. Finally, we draw some conclusions in Section 5.

2 A Morphological Property

In this Section, we assume that data fidelity f is the L^1 norm, i.e, $f(\cdot) = |\cdot|$. Besides we suppose that images take values in $I = [0, L]$, with $L < \infty$ rather than $\mathbb{R}$. We show that under these assumptions the ACWE model yields a contrast invariant filter. The approach followed here is similar to the one proposed in [15] to show that the Total Variation minimization with the L^1 data fidelity term yields a morphological filter. We first introduce the notion of change of contrast before proving the morphological property.

First we define the lower level set u^λ, of an image u with level $\lambda \in I$, as follows $u^\lambda(x) = \mathbb{1}_{u(x)\leq\lambda} \ \forall x \in \Omega$. We follow the work of Guichard and Morel [22] and define a continous change of contrast as any continuous non-decreasing function. We now introduce a lemma proved in [21].

Lemma 1 *Assume that* g *is a continuous change of contrast and* u *is a real function defined on Ω. The following holds for almost all λ:*

$$\exists \mu, \ (g(u))^\lambda = u^\mu \ .$$

In other words, after a change of contrast the structure of the level lines remains the same, only their associated gray levels change. In the sequel, equalities are given for almost all λ. We now reformulate the energy on the level sets of the two variables μ_0 and μ_1. First note that for any $(a, b) \in \mathbb{R}^2$ we have $|a - b| = \int_{\mathbb{R}} |a^\lambda - b^\lambda| d\lambda$. Using the latter equality we get:

$$\begin{aligned} E(\Omega_1, \mu_0, \mu_1 | v) = \beta Per(\Omega_1) & \\ + \int_{\Omega\setminus\Omega_1} \left\{ \int_I |\mu_0^\lambda - v_s^\lambda| d\lambda \right\} & \\ + \int_{\Omega_1} \left\{ \int_I |\mu_1^\lambda - v_s^\lambda| d\lambda \right\} \ . & \end{aligned} \tag{2}$$

By interchanging the integral we have:

$$E(\Omega_1, \mu_0, \mu_1 | v) = \int_I \left\{ \underbrace{\frac{\beta}{L} P(\Omega_1) + \int_{\Omega\setminus\Omega_1} |\mu_0^\lambda - v(x)^\lambda| dx + \int_{\Omega_1} |\mu_1^\lambda - v(x)^\lambda| dx}_{E^\lambda(u, \mu_0^\lambda, \mu_1^\lambda | v^\lambda)} \right\} d\lambda. \tag{3}$$

Finally, we have the reformulation of the whole energy as an integral over gray level values of binary energies associated to each level set:

$$E(u, \mu_0, \mu_1 | v) = \int_I E^\lambda(u, \mu_0^\lambda, \mu_1^\lambda | v^\lambda) d\lambda \ . \tag{4}$$

The next proposition states the contrast invariant property of the ACWE-model with L^1 data fidelity.

Theorem 1 *Let* v *be an observed image and* g *be a continuous change of contrast. Besides assume* $(\hat{u}, \hat{\mu_0}, \hat{\mu_1})$ *is a global minimizer of* $E(\cdot,\cdot,\cdot|v)$*. Then* $(\hat{u}, g(\hat{\mu_0}), g(\hat{\mu_1}))$ *is a global minimizer of* $E(\cdot,\cdot,\cdot|g(v))$.

Proof: Due to the decomposition of the energy on the level sets given by Eq. 4, it is enough to show that for any level $\lambda \in I$, a minimizer for $E(\cdot,\cdot,\cdot|g(v)^\lambda)$ is $(\hat{u}, g(\hat{\mu_0})^\lambda, g(\hat{\mu_1})^\lambda)$. Lemma 1 yeilds the existence of μ such that $v^\mu = g(v)^\lambda$. A minimizer for $E^\mu(\cdot,\cdot,\cdot|v^\mu)$ is $(\hat{u}, \hat{\mu_0}^\mu, \hat{\mu_1}^\mu)$. Since we have $\hat{\mu_i} = g(\hat{\mu_i})^\lambda$, for $i \in \{1,2\}$ we can state that $(\hat{u}, g(\hat{\mu_0})^\lambda, g(\hat{\mu_1})^\mu)$ is a minimizer for $E^\mu(\cdot,\cdot,\cdot|g(v)^\lambda)$. This concludes the proof. □

In other words, the ACWE model with L^1 data fidelity seen as a filter, commutes with any change of contrast. A direct consequence of the latter proposition is that optimal values of μ_0 and μ_1 necessarily belong the set of gray level values which are present in the observed image. To our knowledge this theoretical result is new.

3 An Inclusion Property

In this section, we first discretize the energy defined by Eq. (1). Then we present our main result which describe the behavior of the set Ω_1 of minimizers with respect to the gray levels variables μ_0 and μ_1.

3.1 Discretization and reformulation

For the rest of this paper we assume the following. An image u is defined on a discrete lattice S endowed with a neighborhood system $\mathcal{N}$. We consider a neighborhood defined by the C-connectivity ($C \in \{4, 8\}$). Two neighboring sites s and t are referred to as $s \sim t$. We denote by u_s the value of the pixel at site $s \in S$. Moreover we assume that pixels take value in the discrete set $\{0, \delta, \ldots, L-\delta, L\}$ where $\delta > 0$ is a positive quantization step. Now the set Ω_1 is a subset of the discrete lattice S. We define the binary image u as the *characteristic function* of the set $\Omega \setminus \Omega_1$, i.e., we have:

$$\forall s \in S \;\; u_s = \left(\chi_{\Omega\setminus\Omega_1}\right)_s = \begin{cases} 0 & \text{if } \; s \notin \Omega \setminus \Omega_1 \\ 1 & \text{if } \; s \in \Omega \setminus \Omega_1 \;\; . \end{cases}$$

We approximate locally the perimeter of a set as justified by Boykov *et al.* in [4]. Only pairwise interaction are considered:

$$Per(\Omega_1) = Per(\Omega \setminus \Omega_1) = \sum_{(s,t)} w_{st} \left| u_s - u_t \right| \;\; ,$$

where the coefficients w_{st} are positive constants. The discretization of the data fidelity term f is straightforward. A discrete form of the energy given by Eq. (1)

is thus:

$$E(u,\mu_0,\mu_1) = \beta \sum_{(s,t)} w_{st}|u_s - u_t| + \sum_{s\in S}(1-u_s)\left\{f(\mu_1,v_s) - f(\mu_0,v_s)\right\} + \sum_{s\in S} f(\mu_0,v_s) \ . \tag{5}$$

Now we introduce the new variable K which measures the difference between the two labels μ_0 and μ_1, i.e:

$$\mu_1 = \mu_0 + K \ . \tag{6}$$

Without loss of generality we can assume that $\mu_1 \geq \mu_0$ and thus $K \geq 0$. Instead of considering the energy $E(u,\mu_0,\mu_1)$, we work on the energy $E(u,\mu_0,K)$ defined as follows:

$$E(u,\mu_0,K) = \beta \sum_{(s,t)} w_{st}|u_s - u_t| + \sum_{s\in S} u_s\left\{f(\mu_0,v_s) - f(\mu_0+K,v_s)\right\} + \sum_{s\in S} f(\mu_0+K,v_s) \ . \tag{7}$$

Now assume that K is fixed to some value and define the restricted energy $E^k(u,\mu_0)$ as $E^k(u,\mu_0) = E(u,\mu_0,K)$. In the next Subsection, we give an inclusion property for the energy $\underset{u}{\operatorname{argmin}}\, E^k(u,\cdot)$.

3.2 An inclusion lemma

We first introduce the notion of convexity for a function along with a useful equivalence.

Definition 1 *Let f be a one-dimensional function $f : \mathbb{R} \mapsto \mathbb{R}$. This function if said* convex *if it satisfies one of the two equivalent propositions:*

a) $\forall x \forall y \ \ \forall \theta \in [0,1] \ \ f(\theta x + (1-\theta)y) \leq \theta f(x) + (1-\theta) f(y)$
b) $\forall x \ \forall y \geq x \ \ \forall d \geq 0 \ \ d \leq (y-x) \qquad f(x) + f(y) \geq f(x+d) + f(y-d) \ .$

The proof of the latter equivalence is given in [14]. We endow the space of binary images with the following partial order:

$$a \preceq b \text{ iff } a_s \leq b_s \ \forall s \in S \ .$$

We are now ready to formulate our inclusion property.

Theorem 2 *Assume $\widehat{\mu_0} \leq \widetilde{\mu_0}$. Let us defined the binary images $\widehat{u}$ and $\widetilde{u}$ as minimizers of $E^K(\cdot, \widehat{\mu_0})$ and $E^K(\cdot, \widetilde{\mu_0})$ respectively, i.e:*

$$\widehat{u} \in \min\{u | E^K(u, \widehat{\mu_0})\} \ ,$$
$$\widetilde{u} \in \min\{u | E^K(u, \widetilde{\mu_0})\} \ .$$

Then we have the following inclusion:

$$\hat{u} \preceq \tilde{u} \ . \tag{8}$$

Proof: The proof is an adaptation of the one proposed in [16]. First note that if a and b are two binary variables then we have the following equality $|a-b| = a+b-2ab$. So starting from the energy defined by Eq. (7), the local posterior energy of $E^K(u_s, \mu_0 | v_s, u_t, t \sim s)$ at the site s rewrites as:

$$E^K(u_s, \mu_0 | v_s, u_t, t \sim s) = \phi_s(\mu_0)\, u_s + \psi_s(\mu_0),$$

where

$$\phi_s(\mu_0) = \beta \sum_{t \sim s} w_{st}(1 - 2u_t) + f(\mu_0, v_s) - f(\mu_0 + K, v_s) \ , \tag{9}$$

and

$$\psi_s(\mu_0) = \beta \sum_{t \sim s} w_{st} u_t + f(\mu_0 + K, v_s) \ .$$

Thus the Gibbs local conditional posterior probability [32] is

$$P(u_s = 1 | N_s, \mu_0) = \frac{\exp -\phi_s(\mu_0)}{1 + \exp -\phi_s(\mu_0)} = \frac{1}{1 + \exp \phi_s(\mu_0)} \ .$$

The rest of the proof relies on coupled Markov chains [28, 18]. One can create two Gibbsian samplers of the two posterior distributions for the two level $\hat{\mu_0}$ and $\tilde{\mu_0}$. It is shown in [16] that if $\phi_s(\mu_0)$ is a *non-increasing* function with respect to μ_0 and if $\phi_s(\mu_0)$ does not depend on u_s, then one can devise a coupled Markov chain [28, 18] such that the two distributions are sampled while the inclusion property given by the inequality (8) is preserved. The same result holds using a simulated annealing procedure [19], and thus we get two global minimizers for the two posterior distribtion with the desired inclusion property.

Let us prove that the above assumptions are satisfied. It is easily seen that $\psi_s(\mu_0)$ does not depend on u_s. Thus, it remains to show that $\phi_s(\cdot)$ is a *non-increasing* function. The part $\beta \sum_{t \sim s} w_{st}(1 - 2u_t)$ in Eq. (9) satisfies the *non-increasing* assumption since it does not depend on μ_0. Thus, it only remains to show that for all $\mu_0, \bar{\mu_0}$ such that $\mu_0 \geq \bar{\mu_0}$, we have

$$f(\mu_0) - f(\mu_0 + K) \geq f(\bar{\mu_0}) - f(\bar{\mu_0} + K) \ .$$

This is equivalent to

$$f(\mu_0) + f(\bar{\mu_0} + K) \geq f(\bar{\mu_0}) + f(\mu_0 + K) \ .$$

And the latter corresponds to the convexity of the function f as described in Definition 1-b) with $K \geq 0$ as defined by Eq. (6). This concludes the proof. □

A similar inclusion property has been shown for models involving the Total Variation with convex data fidelity [9, 16, 24, 33]. Proofs in these papers can also be adapted to show Theorem 2. To our knowledge, this inclusion for the discrete binary Mumford-Shah is an original contribution. In the next Section we show how to use this inclusion property to compute a global minimizer.

4 Exact Optimization and Result

This section is devoted to the design of a fast and exact global minimizer of the ACWE-model. It takes benefit from the inclusion property of Lemma 2.

A direct minimization fo the energy $E(u, \mu_0, \mu_1)$ defined by Eq. (5) is a difficult problem. Here we propose an algorithm which computes a global optimizer by solving a family of simpler problems. Assume the two values μ_0 and K are set to some fixed values and we desire to find $\min\{u|E^K(u, \mu_0)\}$. Although this problem is still a non-convex one however it can be solved exactly in variational framework following the work of Chan *et al.* in [10].

Another approach consists of noticing that finding a global minimizer of $E(\cdot, \mu_0, K)$ corresponds to computing a Maximum *a posteriori* estimator of an Ising model [32]. This combinatorial problem can be efficiently computed via tools borrowed from graph theory as originally proposed by Greig *et al.* in [20]. This approach consists of building a graph such that its minimum cost cut (or equivalently its maximum flow [1]) yields an optimal binary configuration which minimizes the energy. Since this seminal work, many graph construction has been devised along with some efficient algorithm to perform the minimum cut. In this paper, we use the graph construction of [25] and the minimum cut algorithm described in [5]. It is shown in [5] that using this latter approach yields a *quasi*-linear algorithm with respect to the number of pixels, although the worst case complexity of the maximum flow algorithm of [5] is exponentiel. We refer to reader to [1, 13] for poynomial maximum-flow algorithms.

A direct algorithm using this minimum cut approach consist of minimizing the energy for all possible values of the couple (μ_0, K) and to keep the couple which gives the lowest energy. We now present two improvements to get better performance.

When K is fixed to some value, we can apply lemma 2 in order to reduce the size of the problem (and thus the size of the graph to build). Indeed, assume that $\hat{u}$ and $\bar{u}$ are two global minimizers associated to the two levels $\hat{\mu_0}$ and $\bar{\mu_0}$ such that $\hat{\mu_0} \leq \bar{\mu_0}$. Then due to Lemma 2 we have $\forall s\, \hat{u}_s = 1 \Rightarrow \bar{u}_s = 1$. Consequently, at the level $\bar{\mu_0}$ it is useless to put into the graph construction a pixel whose value is 1 at the level $\hat{\mu_0}$ (since we already know its value.) Thus we perform a traversal on the discrete set $\{0, \delta, \ldots, L - \delta, L\}$ from the lowest to the highest level, and we keep track of pixels which are already set to 1. This procedure allows for building smaller graphs.

However a much better improvement can be achieved. Instead of keeping track of pixels which can change their values, we keep track of the *connected components* of the pixels which can change their value (i.e., pixels whose value is 0). Due to the pairwise Markovian nature of the interaction in the energy (7), optimization of this energy restricted over two disjoint connected components can be performed *independently* as shown in [16]. The latter procedure yields much smaller graph constructions in practice. Both the tracking of pixels and the connected components updates can be efficiently implemented using Tarjan's Union-Find algorithm [13]. The pseudo-code of the algorithm is described on Figure 1.

$\forall s \in S\ \hat{u}_s \leftarrow 0$
for $(K = 0; K < L; ++K)$
    Reset connected component map
    for $(\mu_0 = 0; (\mu_0 + K) < L; ++\mu_0)$
        $u' \leftarrow \underset{u}{\operatorname{argmin}}\ E^K(u, \mu_0)$
        if $(E^K(u', \mu_0) < E^K(\hat{u}, \mu_0))$
            $\hat{u} \leftarrow u'$
        update connected component map
return $\hat{u}$

Fig. 1. Inclusion-based minimization algorithm.

For the experiments, we have used 4-connectivity, set $w_{st} = 1$ for all interactions, and set the parameters $L = 255$ and $\delta = 1$. The data fidelity is modelled by the L^1-norm.

Figure 2 depicts the original image *cameraman* and *squirrel* along with the optimal results for $\beta = 10$ and a L^1 data fidelity. Using these parameters the optimal values are $\mu_0 = 14$ and $\mu_1 = 159$

Figure 3 depicts the original image *squirrel* with the optimal results for different values of the perimeter regularization coefficient $\beta = 10, 20, 30$. For $\beta = 10$, we obtain $\mu_0 = 64$ and $\mu_1 = 129$ while we get $\mu_0 = 67$ and $\mu_1 = 130$ for both $\beta = 20$ and $\beta = 30$. As expected, the higher β is the more the border of the segmented regions are smooth. Small regions that are observed for low β disappear as the regularization becomes stronger. Note that the result for $\beta = 30$ depicted in Figure 3 presents some blocky region. This behavior is due to the fact that 4-connectivity is used. It can be easily corrected by using better perimeter numerical schemes for perimeter approximation such as those presented in [3, 17].

The complexity of the direct algorithm is $\Theta(L^2 \cdot T(n, m))$ where $T(n, m)$ is the time required to compute a minimum-cut on a graph of n nodes and m edges. Recall that we are using the algorithm proposed by Boykov and Kolmogorov [5] that have a quasi-linear time complexity in practice. For our experiments n is

(a) (b)

Fig. 2. Original image of *cameraman* is depicted in (a) while the optimal minimizer for the ACWE model with L^1-norm as data fidelity and with $\beta = 10$ is shown in (b).

the number of pixels and $m = O(4n)$ since we are using 4-connectivity. The worst case complexity for the inclusion-based algorithm is the one of the direct algorithm. Indeed, the worst case for the inclusion based algorithm happens when no inclusion are present during the optimization process. For instance, a worst case happens when the optimal result is a constant image whose all pixels take the value $(L-1)$. However, for natural images this scenario is highly improbable. Time results (on a 3GHz Pentium IV) of the two minimization algorithms for the ACWE model with L^1 data fidelity, on different size of the image *cameraman*, and with different weighted coefficient β, are presented in Table 1. As one can see, both algorithms have a small dependence with the weighted coefficient β. In practice, both of them have a quasi-linear behavior with respect to the number of pixels. The same kind of results were obtained for the *squirrel* image. The gain we obtain using the inclusion-based algorithm compared to the direct approach varies from about 3 (for 32^2 size image) to about 4 (for 256^2 size images). Further studies need to be done to understand this behavior.

5 Conclusion

We have presented new results on the analysis of the binary Mumford-Shah model. In particular we have shown that it yields a contrast invariant filter if L^1 data fidelity is used. Besides, we have shown an inclusion of the minimizers. The latter has been used to propose an efficient algorithm which computes an exact minimizer.

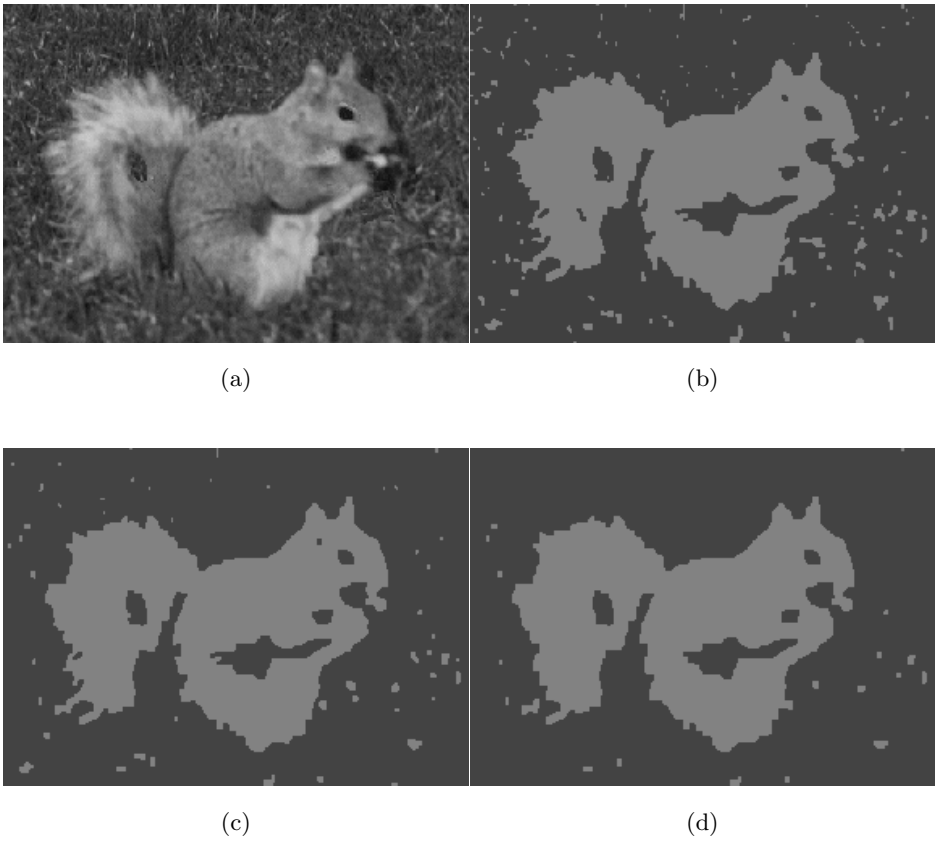

(a) (b)

(c) (d)

Fig. 3. Original image of *squirrel* is depicted in (a) while the optimal minimizer for the ACWE model with L^1-norm as data fidelity for $\beta = 10, 25$ and 30 are respectively shown in (b), (c) and (d).

Comparisons with non optimal schemes such as the ones described in [7, 8, 12] remain to be done. This will be presented in a forthcoming paper along with another algorithm which also takes benefit from the inclusion property of the minimizers.

Acknowledgements

The author thanks Marc Sigelle form Ecole Nationale des Télćommunications (ENST) and Antonin Chambolle from CMAP Ecole Polytechnique for fruitfull discussions. The author also thanks Ali Haddad and Guy Gilboa from UCLA for nice suggestions and careful last minute proofreading. Any remaining errors are of course my own.

Table 1. Time results in seconds (on a 3GHz Pentium IV) of the direct (inside parentheses) and inclusion-based algorithms for different weight coefficient β and different size of the image *cameraman*.

Size	$\beta = 5$	$\beta = 10$	$\beta = 15$
32^2	4.16 (13.1)	4.4 (13.8)	4.8 (14.6)
64^2	17.1 (54.3)	17.8 (57.5)	18.5 (60.7)
128^2	72.57(243.3)	77.2 (254.6)	81.1 (268.4)
256^2	364.8 (1813.4)	382.2 (1851.7)	414.3 (2081.6)

References

1. R.K Ahuja, T.L. Magnanti, and J.B. Orlin. *Network Flows: Theory, Algorithms and Applications*. Prentice Hall, 1993.
2. G. Aubert and P. Kornprobst. *Mathematical Problems in Image Processing*. Springer-Verlag, 2002.
3. Y. Boykov and M.-P Jolly. Interactive graph cuts for optimal boundary and region segmentation of objects in n-d images. In *Proceedings of International Conference on Computer Vision*, pages 105–112, 2001.
4. Y. Boykov and V. Kolmogorov. Computing geodesic and minimal surfaces via graph cuts. In *International Conference on Computer Vision*, volume 1, pages 26–33, 2003.
5. Y. Boykov and V. Kolmogorov. An experimental comparison of min-cut/max-flow algorithms for energy minimization in vision. *IEEE Transactions on Pattern Analysis and Machine Intelligence*, 26(9):1124–1137, 2004.
6. Y. Boykov, O. Veksler, and R. Zabih. Fast approximate energy minimization via graph cuts. *IEEE Transactions on Pattern Analysis and Machine Intelligence*, 23(11):1222–1239, 2001.
7. X. Bresson, S. Esedoglu, P. Vandergheynst, J.P. Thiran, and S. Osher. Global minimizers of the active contour/snake model. Technical Report 05-04, UCLA CAM Report, 2005.
8. V. Caselles and A. Chambolle. Anistropic curvature-driven flow of convex sets. Technical Report 528, CMAP Ecole Polytechnique, 2004.
9. A. Chambolle. Total variation minimization and a class of binary mrf models. In *Energy Minimization Methods in Computer Vision and Pattern Recognition*, volume LNCS 3757, pages 136 – 152, St. Augustine, Florida, USA, 2005.
10. T. F. Chan, S. Esedoglu, and M. Nikolova. Finding the global minimum for binary image restoration. In *Proceedings of the ICIP 2005*, pages 121–124, Genova, Italy, 2005.
11. T.F. Chan, S. Esedoglu, and M. Nikolova. Algorithms for Finding Global Minimizers of Image Segmentation and Denoising Models. Technical Report 54, UCLA, 2004.
12. T.F. Chan and L. Vese. Active contours without edges. *IEEE Transactions on Image Processing*, 10(2):266–277, 2002.
13. T.H. Cormen, C.E. Leiserson, R.L. Rivest, and C. Stein. *Introduction to Algorithms*. The MIT Press, 2001.
14. J. Darbon. *Composants Logiciels et Algorithmes de minimisation exacte d'énergies dédiś au traitement des images*. PhD thesis, Ecole Nationale Supérieure des Télécommunications, October 2005.

15. J. Darbon. Total Variation minimization with L^1 data fidelity as a contrast invariant filter. In *Proceedings of the 4th IEEE International Symposium on Image and Signal Processing and Analysis (ISPA 2005)*, Zagreb, Croatia, September 2005.
16. J. Darbon and M. Sigelle. A fast and exact algorithm for Total Variation minimization. In *Proceedings of the 2nd Iberian Conference on Pattern Recognition and Image Analysis (IbPRIA)*, volume 3522, pages 351–359, Estoril, Portugal, June 2005. Springer-Verlag.
17. J. Darbon and M. Sigelle. Image restoration with discrete constrained Total Variation part I: Fast and exact optimization. *Journal of Mathematical Imaging and Vision, Online First*, 2005.
18. P.M. Djurić, Y. Huang, and T. Ghirmai. Perfect sampling : A review and applications to signal processing. *IEEE Signal Processing*, 50(2):345–256, 2002.
19. S. Geman and D. Geman. Stochastic relaxation, Gibbs distributions, and the bayesian restoration of images. *IEEE Transactions on Pattern Analysis and Machine Intelligence*, 6(6):721–741, 1984.
20. D. Greig, B. Porteous, and A. Seheult. Exact maximum a posteriori estimation for binary images. *Journal of the Royal Statistics Society*, 51(2):271–279, 1989.
21. F. Guichard and J.-M. Morel. *Image Iterative Smoothing and PDE's.* please write email to fguichard@poseidon-tech.com, 2000.
22. F. Guichard and J.M. Morel. Mathematical morphology "almost everywhere". In *the Proceedings of Internationnal Symposium on Mathematical Morpholy*, pages 293–303. CSIRO Publishing, April 2002.
23. L. He and S. Osher. Solving the chan-vese model by a multuphase level set algorithm based on the topological derivative. Technical Report CAM 06-56, University of California, Los Angeles (UCLA), October 2006.
24. D. S. Hochbaum. An efficient algorithm for image segmentation, markov random fields and related problems. *Journal of the ACM*, 48(2):686–701, 2001.
25. V. Kolmogorov and R. Zabih. What energy can be minimized via graph cuts? *IEEE Transactions on Pattern Analysis and Machine Intelligence*, 26(2):147–159, 2004.
26. D. Mumford and J. Shah. Optimal approximation by piecewise smooth functions and associated variational problems. *Comm. on Pure and Applied Mathematics*, 42:577–685, 1989.
27. S. Osher and N. Paragios, editors. *Geometric Level Set Methods*. Springer, 2003.
28. J. G. Propp and D. B. Wilson. Exact sampling with coupled Markov chains and statistical mechanics. *Random Structures and Algorithms*, 9(1):223–252, 1996.
29. J. Serra. *Image Analysis and Mathematical Morphology*. Academic Press, 1988.
30. B. Song and T.F. Chan. A fast algorithm for level set based optimization. Technical Report CAM 02-68, University of California, Los Angeles (UCLA), December 2002.
31. L. Vese and T.F. Chan. A mutiphase level set framework for image segmentation using the Mumford-Shah model. *International Journal of Computer Vision*, 50(3):266–277, 2002.
32. G. Winkler. *Image Analysis, Random Fields and Dynamic Monte Carlo Methods*. Applications of mathematics. Springer-Verlag, 2^{nd} edition, 2003.
33. B.A. Zalesky. Network Flow Optimization for Restoration of Images. *Journal of Applied Mathematics*, 2:4:199–218, 2002.